Human Molecular Genetics, 2018, Vol. 27, No. 15 2712–2724

doi: 10.1093/hmg/ddy181
Advance Access Publication Date: 14 May 2018
Original Article

ORIGINAL ARTICLE

BHD-associated kidney cancer exhibits unique molecular characteristics and a wide variety of variants in chromatin remodeling genes

Hisashi Hasumi[1,2,*,†], Mitsuko Furuya[3,†], Kenji Tatsuno[4], Shogo Yamamoto[4], Masaya Baba[2,5], Yukiko Hasumi[2,6], Yasuhiro Isono[7], Kae Suzuki[1], Ryosuke Jikuya[1], Shinji Otake[1], Kentaro Muraoka[1], Kimito Osaka[1], Narihiko Hayashi[1], Kazuhide Makiyama[1], Yasuhide Miyoshi[1], Keiichi Kondo[1], Noboru Nakaigawa[1], Takashi Kawahara[1], Koji Izumi[1], Junichi Teranishi[1], Yasushi Yumura[1], Hiroji Uemura[1], Yoji Nagashima[8], Adam R. Metwalli[2], Laura S. Schmidt[2,9], Hiroyuki Aburatani[4], W. Marston Linehan[2] and Masahiro Yao[1,*]

[1]Department of Urology, Yokohama City University, Yokohama 236-0004, Japan, [2]Urologic Oncology Branch, Center for Cancer Research, National Cancer Institute, National Institutes of Health, Bethesda, MD, USA, [3]Department of Molecular Pathology, Yokohama City University, Yokohama 236-0004, Japan, [4]Genome Science Division, Research Center for Advanced Science and Technology, The University Tokyo, Tokyo 153-8904, Japan, [5]International Research Center for Medical Sciences, Kumamoto University, Kumamoto 860-0811, Japan, [6]Department of Ophthalmology, [7]Department of Otorhinolaryngology, Yokohama City University, Yokohama 236-0004, Japan, [8]Department of Surgical Pathology, Tokyo Women's Medical University, Tokyo 162-8666, Japan and [9]Basic Science Program, Leidos Biomedical Research, Inc., Frederick National Laboratory for Cancer Research, Frederick, MD, USA

*To whom correspondence should be addressed at: Department of Urology, Yokohama City University, 3-9 Fuku-ura, Kanazawa-ku, Yokohama 2360004, Japan. Tel: +81 457872679; Fax: +81 45786511; Email: hasumi@yokohama-cu.ac.jp (H.H.); Email: masayao@yokohama-cu.ac.jp (M.Y.)

Abstract

Birt–Hogg–Dubé (BHD) syndrome is a hereditary kidney cancer syndrome, which predisposes patients to develop kidney cancer, cutaneous fibrofolliculomas and pulmonary cysts. The responsible gene *FLCN* is a tumor suppressor for kidney cancer, which plays an important role in energy homeostasis through the regulation of mitochondrial oxidative metabolism. However, the process by which *FLCN*-deficiency leads to renal tumorigenesis is unclear. In order to clarify molecular pathogenesis of BHD-associated kidney cancer, we conducted whole-exome sequencing analysis using next-generation sequencing technology as well as metabolite analysis using liquid chromatography–mass spectrometry and gas

[†]These authors contributed equally to this work.
Received: December 4, 2017. **Revised:** May 2, 2018. **Accepted:** May 8, 2018

chromatography–mass spectrometry. Whole-exome sequencing analysis of BHD-associated kidney cancer revealed that copy number variations of BHD-associated kidney cancer are considerably different from those already reported in sporadic cases. In somatic variant analysis, very few variants were commonly observed in BHD-associated kidney cancer; however, variants in chromatin remodeling genes were frequently observed in BHD-associated kidney cancer (17/29 tumors, 59%). Metabolite analysis of BHD-associated kidney cancer revealed metabolic reprogramming toward upregulated redox regulation which may neutralize reactive oxygen species potentially produced from mitochondria with increased respiratory capacity under *FLCN*-deficiency. BHD-associated kidney cancer displays unique molecular characteristics that are completely different from sporadic kidney cancer, providing mechanistic insight into tumorigenesis under *FLCN*-deficiency as well as a foundation for development of novel therapeutics for kidney cancer.

Introduction

Birt–Hogg–Dubé (BHD) syndrome is an inherited kidney cancer syndrome which predisposes patients to develop hair follicle tumors, lung cysts, spontaneous pneumothorax and an increased risk of renal neoplasia with a spectrum of histologic tumor types, including hybrid oncocytic/chromophobe tumor (HOCT), chromophobe renal cell carcinoma (chRCC), oncocytoma, papillary renal cell carcinoma (pRCC) and clear cell renal cell carcinoma (ccRCC) (1,2). In 2002, germline mutation in the *folliculin (FLCN)* gene was identified in BHD patients. Most of these mutations are frameshift or nonsense mutation with an exon 11 'hot spot' in a tract of eight cytosines (C8) (3). Missense mutations in *FLCN* including H255Y and K508R have been described, but occur less frequently (4). Multiple renal tumors from a single BHD patient have different somatic second hit mutations in the *FLCN* gene, supporting multifocal development of BHD-associated kidney cancer (5).

Folliculin (FLCN) encoded by the *FLCN* gene was a completely unknown protein with no known functional domains at the time of its discovery. However, subsequent studies have uncovered a variety of metabolic functions for FLCN. FLCN controls energy homeostasis by regulating the 5′-AMP activated protein kinase/mammalian target of rapamycin (mTOR) pathway and peroxisome proliferative activated receptor, gamma, coactivator 1α (*PGC1a*) driven mitochondrial oxidative metabolism (6–14). FLCN binds to two partner proteins, FLCN-interacting proteins 1 (FNIP1) and 2 (FNIP2). The interaction between FLCN and FNIP1/FNIP2 is a critical element for the FLCN/FNIP1/FNIP2 complex to exert tumor suppressive functions and to control energy homeostasis by regulating *PGC1a*-driven mitochondrial oxidative metabolism (15–19).

Whole-body heterozygous *Flcn* knockout mice developed kidney tumors at 18 months of age that demonstrated loss of heterozygosity (LOH) at the *Flcn* locus. This *Flcn*-deficient phenotype mimics BHD-associated kidney cancer and highlights *FLCN* as a classical tumor suppressor inactivated by two mutational events (20). On the other hand, mice in which *Flcn* is homozygously inactivated in the kidney developed enlarged polycystic kidneys with hyperplastic cells protruding into the cystic lumen, and died at 3 weeks of age owing to renal failure prior to the formation of kidney tumors (21). These data suggest that additional genetic alterations in addition to *FLCN* mutation may be necessary for the development of BHD-associated kidney cancer.

To investigate additional variants in BHD-associated kidney cancer, whole-exome sequencing analysis of BHD-associated kidney cancer was performed. In addition, metabolite analysis was carried out to further understand the molecular pathogenesis of BHD-associated kidney cancer. These analyses uncovered unique molecular characteristics that are completely different from sporadic kidney cancer, and revealed metabolic reprogramming of BHD-associated kidney cancer toward upregulated redox regulation which may protect *FLCN*-deficient tumor cells from reactive oxygen species potentially produced from abundant mitochondria under *FLCN*-deficiency.

Results

Germline *FLCN* mutations of BHD patients and diverse histology of BHD-associated kidney cancer

To elucidate the molecular pathogenesis of BHD-associated kidney cancer, whole-exome sequencing was performed using 29 BHD-associated kidney tumors from 15 BHD patients whose *FLCN* germline mutations were already confirmed by Sanger sequencing. Most *FLCN* germline mutations were frameshift including an in/del mutation in the mutational 'hot spot' in the C8 tract of Exon 11 observed in 6 patients and nonsense mutations. Amino acid deletions without frameshift were detected in two cases and exon skipping without frameshift in one case (Table 1). Pathologic findings revealed renal tumors with diverse histologies including 5 HOCTs, 15 chRCC, three HOCT or chRCC not determined owing to postmortem degradation, 1 oncocytoma, 2 ccRCC, 2 pRCC and 1 tubulopapillary renal cell carcinoma (Tub pap) (Table 2; Fig. 1).

Second hits in the *FLCN* gene in BHD-associated kidney cancer

Whole-exome sequencing of BHD-associated kidney cancers detected somatic *FLCN* mutations in 25 out of the 29 renal tumors; 20 tumors showed frameshift/nonsense mutations or LOH in the remained *FLCN* allele. Interestingly, four tumors showed missense mutations including G84C, W260L, L356P and L550R, suggesting that these altered residues may affect the tumor suppressive function of the FLCN protein (Table 2).

Copy number variation in BHD-associated kidney cancer

Using whole-exome sequencing data, we investigated copy number variation (CNV) in BHD-associated kidney cancer. We observed less CNV in HOCT, chRCC and oncocytoma compared with ccRCC and pRCC (Fig. 2), which might reflect the indolent nature of HOCT, chRCC and oncocytoma. In BHD-associated ccRCC, we did not observe loss of chromosome 3p, which is characteristic of sporadic ccRCC (22), indicating that the molecular context of BHD-associated ccRCC might differ from that of sporadic ccRCC.

Somatic variants in BHD-associated kidney cancer

Next, we investigated other somatic variants in BHD-associated kidney cancer using Karkinos4.1.11 software (23). It has been

Table 1. Germline *FLCN* mutations of BHD patients

Patient No.	Germline FLCN mutation	Mutation type
1	c.332_349delACCCCAGCCA CCCCCAGC	Amino acid deletion
2	c.1528_1530delGAG	Amino acid deletion
3	c.1285dupC	Frameshift
4	c.1429 C>T	Nonsense
5	c.1285dupC	Frameshift
6	c.1285dupC	Frameshift
7	c.1285dupC	Frameshift
8	c.199 dupG	Frameshift
9	c.1533_1536delGATG	Frameshift
10	c.1533_1536delGATG	Frameshift
11	c.1347_1353dupCCACCCT	Frameshift
12	c.1347_1353dupCCACCCT	Frameshift
13	c.1285dupC	Frameshift
14	c.397-1G>C	Exon deletion
15	c.1285dupC	Frameshift

Numbering according to GenBank Accession No. NM_144997.5 with A of initiator codon designated as nucleotide1.

reported that sporadic ccRCC/pRCC harbors increased numbers of somatic variants compared with sporadic chRCC/oncocytoma (24). Interestingly, we did not observe any difference in the number of somatic variants between HOCT/chRCC/oncocytoma and ccRCC/pRCC (average somatic variant number, HOCT/chRCC/oncocytoma versus ccRCC/pRCC, 20 versus 23, respectively, $P = 0.77$) (Table 2), further supporting that the molecular context of BHD-associated kidney cancer might differ from that of sporadic cases. Although very few variants were commonly observed across 29 tumors, variants in chromatin remodeling genes were frequently observed (59% of cases) in BHD-associated kidney cancer (Fig. 3), supporting that alterations in chromatin remodeling genes might be critical driver mutations for renal tumorigenesis in BHD. Although we did not observe any variant in tumor suppressors associated with kidney cancer, we observed variants in genes associated with tumor suppressive pathways including p53 pathway, smad pathway and Hippo-Yap pathway (14, 17 and 14%, respectively), suggesting that these pathways are critical for suppression of renal tumorigenesis (Fig. 4). Because *FLCN* plays an important role in metabolism including oxidative phosphorylation, we investigated

Table 2. Somatic second hit *FLCN* mutation in BHD-associated kidney cancer

Patient No.	Tumor No.	Histology	Somatic second hit FLCN mutation	Mutation type	Allele frequencies	Tumor size (mm)	Number of somatic variants
1	4T3	HOCT	c.453_454delGT	Frameshift	0.26	25	16
	4T4	HOCT	c.165delC	Frameshift	0.30	12	22
2	59T8	HOCT	c.1429C>T	Nonsense	0.23	32	18
	59T10	HOCT	c.1649T>G	Missense (p.L550R)	0.19	10	7
	59T11	HOCT	c.278delC	Frameshift	0.24	10	13
	59T1	chRCC	c.1383C>T	Silent	0.34	43	20
	59T2	chRCC	c.779G>T	Missense (p.W260L)	0.32	14	18
	59T3	chRCC	Undetectable	Undetectable	NA	8	8
	59T4	chRCC	c.1285dupC	Frameshift	0.27	9	11
	59T6	chRCC	c.250G>T	Missense (p.G84C)	0.13	17	11
	59T12	chRCC	c.1301delA	Frameshift	0.10	8	7
	59T14	chRCC	Undetectable	Undetectable	NA	14	15
	59T15	chRCC	c.1067T>C	Missense (p.L356P)	0.21	19	92
3	24T1	chRCC	c.1421delC	Frameshift	0.19	30	17
4	35T1	chRCC	c.1234_1235insAG	Frameshift	0.21	10	29
5	38T1	chRCC	c.34G>T	Nonsense	0.36	15	18
6	42T1	chRCC	LOH	LOH	NA	30	21
	42T2	chRCC	c.812delA	Frameshift	0.33	13	21
7	43T1	chRCC	c.673delG	Frameshift	0.14	24	17
8	51T1	chRCC	c.1285dupC	Frameshift	0.26	20	17
9	19T1	Ho/chRCC	c.998C>G	Nonsense	0.17	28	15
	19T2	Ho/chRCC	c.1422_1423insT	Frameshift	0.21	30	18
	19T3	Ho/chRCC	c.543C>A	Nonsense	0.37	13	42
10	98T1	Onco	c.346C>T	Nonsense	0.36	41	14
11	44T1	ccRCC	Undetectable	Undetectable	NA	40	9
12	107T1	ccRCC	c.922G>T	Nonsense	0.41	50	49
13	15T1	pRCC	LOH	LOH	NA	100	12
14	76T1	pRCC	LOH	LOH	NA	140	22
15	85T1	Tub pap	Undetectable	Undetectable	NA	95	13

Numbering according to GenBank Accession No. NM_144997.5 with A of initiator codon designated as nucleotide 1.

HOCT, hybrid oncocytic/chromophobe tumor; chRCC, chromophobe renal cell carcinoma; Ho/chRCC, HOCT or chRCC not determined owing to postmortem degradation; Onco, oncocytoma; ccRCC, clear cell renal cell carcinoma; pRCC, papillary renal cell carcinoma; Tub pap, tubulopapillary renal cell carcinoma; LOH, loss of heterozygosity; NA, not available.

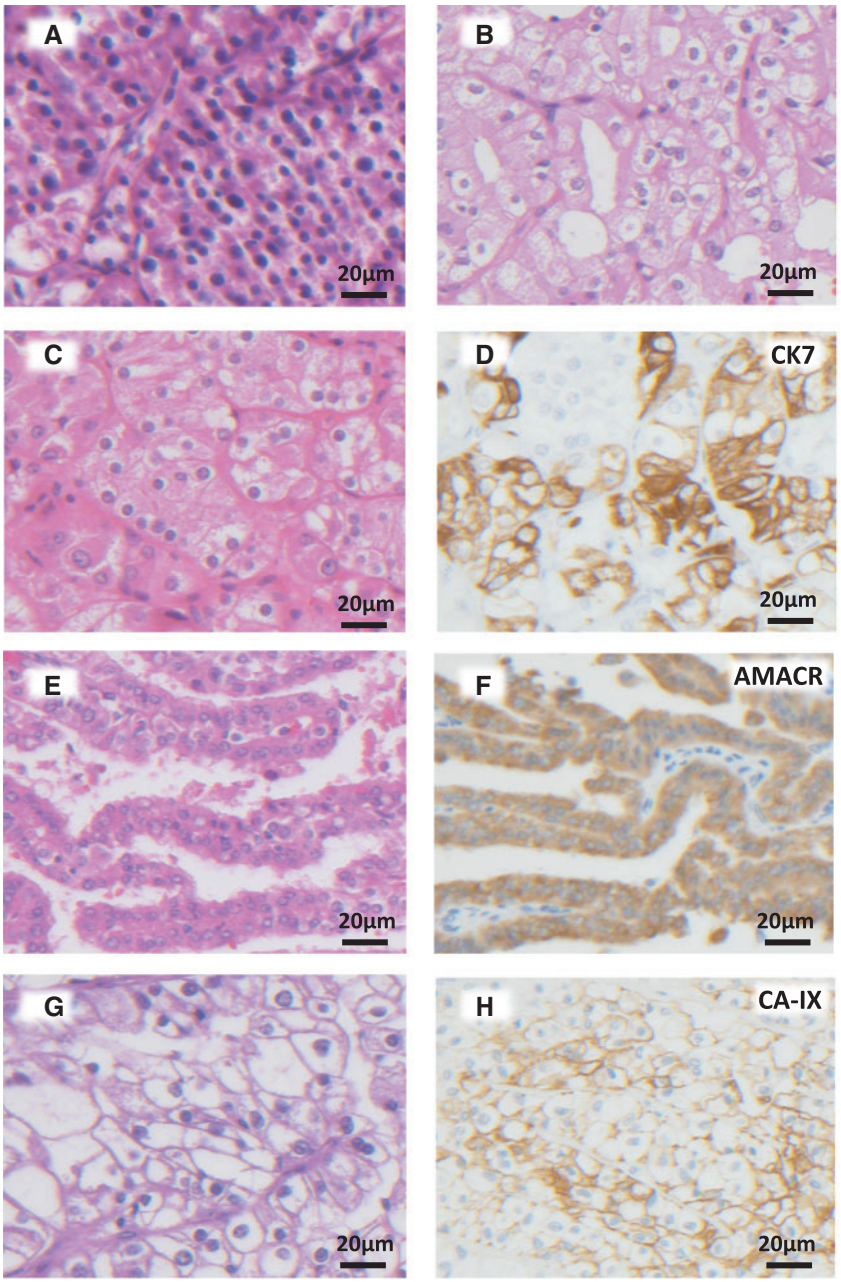

Figure 1. Histology of BHD-associated kidney cancer. (**A**) Oncocytoma (Patient No. 10). (**B**) chRCC (Patient No. 6). (**C**) HOCT (Patient No. 1). (**D**) Tumor cells were positively immunostained for cytokeratin 7 (CK7), suggesting that they were derived from distal tubules or collecting ducts (Patient No. 1). (**E**) pRCC (Patient No. 13). (**F**) Tumor cells were positively immunostained for α-methylacyl-CoA (AMACR), supporting the histology of pRCC (Patient No. 13). (**G**) ccRCC (Patient No. 12). (**H**) Tumor cells were positively immunostained for CA-IX, supporting the histology of ccRCC (Patient No. 12).

variants in genes associated with metabolism. Variants in genes associated with the mitochondrial pathway, lipid metabolism and glycolytic pathway were observed in 28, 24 and 7% of cases, respectively (Fig. 5), suggesting that these metabolic pathways might be altered in BHD-associated kidney cancer.

Metabolic alteration in BHD-associated kidney cancer

To further understand the molecular pathogenesis of BHD-associated kidney cancer, we conducted metabolite analysis using LC/MS spectrometry. Glucose was accumulated in BHD-associated kidney cancer, whereas glycolytic downstream metabolites including glucose 6-phosphate, fructose 6-phosphate, fructose 1,6-bisphosphate, dihydroxyacetone phosphate(DHAP), 3-phosphoglycerate, 2-phosphoglycerate and phosphoenolpyruvate were not significantly increased, indicating that the utilization of glucose might be decreased and thus, BHD-associated kidney cancer might not rely on glycolysis as a main source for energy production (Fig. 6A). Notably, BHD-associated kidney cancer demonstrated increased monoacylglycerols including 2-palmitoylglycerol, 2-oleoylglycerol and 1-linoleoylglycerol as well as increased free fatty acids including palmitoleate, palmitate, arachidate, eicosenoate, non-adecanoate and oleate, suggesting that lipolysis might be upregulated in BHD-associated kidney cancer (Fig. 6B;

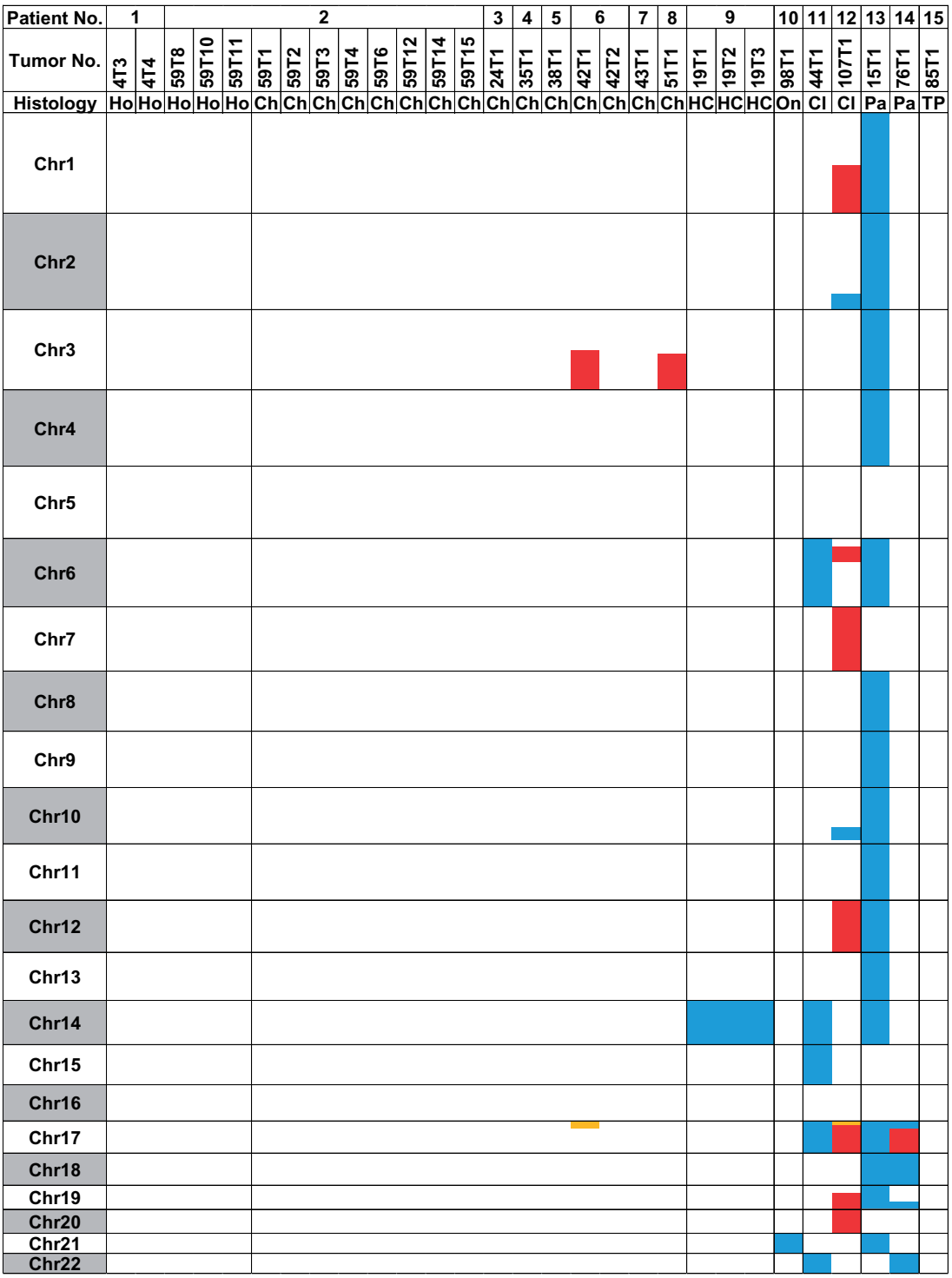

Figure 2. Copy number variation (CNV) of BHD-associated kidney cancer. Blue, red, orange bars indicate copy loss, copy gain, uniparental disomy (UPD), respectively. Ho, HOCT; Ch, chRCC; HC, HOCT or Ch not determined owing to postmortem degradation; On, Oncocytoma; Cl, ccRCC; Pa, pRCC; TP, tubulopapillary renal cell carcinoma.

Supplementary Material, Fig. S3). Furthermore, acyl-carnitines including palmitoylcarnitine, octanoylcarnitine and lauroylcarnitine were increased in BHD-associated kidney cancer, suggesting that the transportation of fatty acids into mitochondria might be facilitated in BHD-associated kidney cancer. Trichloroacetic acid (TCA) cycle metabolites, fumarate and malate were decreased while other TCA metabolites were unchanged, indicating that reductive carboxylation might be upregulated toward lipid synthesis or TCA cycle flux might be higher in BHD-associated kidney cancer (Fig. 6C). Previously, we demonstrated that *FLCN*-deficiency upregulates mitochondrial oxidative metabolism through *PGC1a*, a key co-activator for mitochondrial biogenesis (10). Taken together,

Pathway	Patient No.	1		2												3	4	5	6		7	8	9			10	11	12	13	14	15
	Tumor No.	4T3	4T4	59T8	59T10	59T11	59T1	59T2	59T3	59T4	59T6	59T12	59T14	59T15	24T1	35T1	38T1	42T1	42T2	43T1	51T1	19T1	19T2	19T3	98T1	44T1	107T1	15T1	76T1	85T1
	Histology	Ho	Ho	Ho	Ho	Ho	Ch	Ch	Ch	Ch	Ch	Ch	Ch	Ch	Ch	Ch	Ch	Ch	Ch	Ch	Ch	HC	HC	HC	On	Cl	Cl	Pa	Pa	TP
Chromatin remodeling	ARID1B																													0.5
Chromatin remodeling	ARID3B					0.7																								
Chromatin remodeling	BAHCC1		0.5																											
Chromatin remodeling	BAZ1A																							0.2						
Chromatin remodeling	BAZ2B																	0.6												
Chromatin remodeling	CREBBP															0.8														
Chromatin remodeling	DOT1L																									0.2				
Chromatin remodeling	EID1																												0.6	
Chromatin remodeling	HIST1H1D												0.5																	
Chromatin remodeling	HIST1H2AB																				0.5									
Chromatin remodeling	HMGXB4			1																										
Chromatin remodeling	ING2							0.4																						
Chromatin remodeling	JARID2													0.3																
Chromatin remodeling	MLL2																								0.8					
Chromatin remodeling	NCOR2																				0.1									
Chromatin remodeling	PHF17																										0.5			
Chromatin remodeling	SAP130																			1										
Chromatin remodeling	SETD7																							0.4						
Chromatin remodeling	SMARCAL1																		0.6											
Chromatin remodeling	SMARCD3																										0.2			
Chromatin remodeling	SUPT7L																					0.5								
Chromatin remodeling	TOX3																												0.2	
Chromatin remodeling	ZZZ3							0.7																						
DNA methylation	DIP2B								0.8																					
DNA methylation	GLYR1													0.4																
DNA repair	PDS5B			1																							0.4			
DNA repair	ATAD5		1																											
DNA repair	BOD1L						1																							
DNA repair	RHNO1																					0.5								
DNA repair	FAAP100		1																											
DNA repair	CREBBP															0.8														
DNA repair	DFNA5													0.4																
DNA repair	DTX3L													0.4																
DNA repair	ERCC2																		0.2											
DNA repair	HLTF																		0.6											
DNA repair	HUWE1																								0.8					
DNA repair	MSH3																	0.9												
DNA repair	RAD23A															0.4														
DNA repair	SMC1A							0.5																						
DNA repair	TELO2																					0.3								
DNA repair	TONSL				0.7																									
DNA repair	TOPBP1																										0.3			
DNA repair	UIMC1													0.8																
Telomere regulation	TERB1															1														
Telomere regulation	RTEL1									0.5																				
Telomere regulation	TNKS																												0.5	
Telomere regulation	WRAP53																1													

Figure 3. Somatic variants observed in BHD-associated kidney cancer in genes associated with chromatin remodeling, DNA methylation, DNA repair and telomere regulation. Ho, HOCT; Ch, chRCC; HC, HOCT or Ch not determined owing to postmortem degradation; On, Oncocytoma; Cl, ccRCC; Pa, pRCC; TP, tubulopapillary renal cell carcinoma. Values indicate allele frequencies of variants adjusted by tumor purity calculated by an in-house genotyper, Karkinos4.1.11 (23).

these data suggest that BHD-associated kidney cancer might have more rapid respiratory rate, where carbon flux is increased and the metabolites are oxidized to carbon dioxide more rapidly. In support of these observations, BHD-associated kidney cancer demonstrated increased metabolites in pentose phosphate pathway including ribulose 5-phosphate, ribulose, ribose 5-phosphate, sedoheptulose 7-phosphate and ribose, suggesting that pentose phosphate pathway might be upregulated in order to produce NADPH which is a critical neutralizer for reactive oxygen species produced from active electron transport chain under *FLCN*-deficiency (Fig. 7A). In addition, BHD-associated kidney cancer demonstrated increased metabolites in glutathione (GSH) synthetic pathway including reduced GSH, oxidized glutathione (GSSG), cysteine–glutathione disulfide and ophthalmate, which is a critical pathway for antioxidation, further supporting that redox regulation is crucial for *FLCN*-deficient cells to survive under mitochondria-rich conditions (Fig. 7B).

Discussion

Here, we uncover the genomic and metabolic landscape of kidney cancer, which develops in BHD syndrome, a hereditary kidney cancer syndrome caused by mutation of *FLCN*, a tumor suppressor for kidney cancer. Somatic second hit mutations of *FLCN* were detected in most BHD-associated kidney cancer, highlighting *FLCN* as a classical tumor suppressor inactivated by two hits. CNV in BHD-associated kidney cancer differed depending on each histology; BHD-associated HOCT, chRCC and

Pathway	Patient No.	1		2												3	4	5	6		7	8	9			10	11	12	13	14	15
	Tumor No.	4T3	4T4	59T8	59T10	59T11	59T1	59T2	59T3	59T4	59T6	59T12	59T14	59T15		24T1	35T1	38T1	42T1	42T2	43T1	51T1	19T1	19T2	19T3	98T1	44T1	107T1	15T1	76T1	85T1
	Histology	Ho	Ho	Ho	Ho	Ho	Ch	Ch	Ch	Ch	Ch	Ch	Ch	Ch		Ch	Ch	Ch	Ch	Ch	Ch	Ch	HC	HC	HC	On	Cl	Cl	Pa	Pa	TP
p53 pathway	COPS8													0.4																	
p53 pathway	RFWD2																0.4														
p53 pathway	USP7				1																										
p53 pathway	ZNF385A																											0.5			
smad pathway	ACVR1B						0.5	0.5	0.5																						
smad pathway	RNF111																								0.5						
smad pathway	USP9Y			1																											
Hippo-Yap pathway	AJUBA																								1						
Hippo-Yap pathway	WTIP			0.4																											
Hippo-Yap pathway	WWC2																											0.3			
Hippo-Yap pathway	WWC3																									0.3					
VHL-HIF pathway	LIMD1																													0.2	0.7
Cell cycle	CDC27					1																									
Cell cycle	FBXW7						1																								
Cell development	TSPAN4																														0.5
Genome stability	NUDT18																												0.1		
Genome stability	PAXIP1															0.3															
Microenvironment	DSP																				1										
Microenvironment	KLK10																										0.2				
Microenvironment	LAMA2					1																									
Microenvironment	PKD1																													0.5	
Neuronal regulation	PPP1R9B															0.2															
Splicing factor	RBM10					0.5																									
Splicing factor	SF1																												0.8		
Transcription factor	BNC2													1																	

Figure 4. Somatic variants observed in BHD-associated kidney cancer in genes associated with tumor suppressive pathways including p53 pathway, smad pathway, Hippo-Yap pathway and VHL-HIF pathway. Ho, HOCT; Ch, chRCC; HC, HOCT or Ch not determined owing to postmortem degradation; On, Oncocytoma; Cl, ccRCC; Pa, pRCC; TP, tubulopapillary renal cell carcinoma. Values indicate allele frequencies of variants adjusted by tumor purity calculated by an in-house genotyper, Karkinos4.1.11 (23).

oncocytoma exhibited less CNV compared with BHD-associated ccRCC and pRCC. Somatic variant analysis using Karkinos4.1.11 software revealed frequent variants in chromatin remodeling genes in BHD-associated kidney cancer. Metabolite analysis of BHD-associated kidney cancer revealed a metabolic reprogramming toward glycolysis that constantly feeds the pentose phosphate pathway, an important pathway for redox regulation, and upregulated lipid biosynthesis that may contribute to the development of lipid bilayers in *FLCN*-deficient tumor cells.

The Cancer Genome Atlas (TCGA) project revealed that sporadic chRCC shows copy loss of Chromosome 1, 2, 6, 10, 13 and 17 as well as variants in *TP53*, *CDKN1A*, *RB1*, *PTEN*, *MTOR* and *NRAS* (25). However, 15 cases of BHD-associated chRCC in this study showed very few CNVs and did not reveal any gene variants that were reported in sporadic chRCC in the TCGA project, suggesting that BHD-associated chRCC might have a different molecular pathogenesis from that of sporadic chRCC. Variants in components of the VHL complex, loss of chromosome 3p and variants in chromatin remodeling genes are frequently observed in sporadic ccRCC (26,27). Gain of Chromosome 7 and chromatin remodeling gene variants are reported in sporadic pRCC (28). Although our sample size is small, BHD-associated ccRCC and pRCC did not show any of the molecular characteristics reported in the TCGA project, suggesting that BHD-associated ccRCC and pRCC might have a distinct molecular pathogenesis that is different from that of sporadic ccRCC and pRCC.

Next generation sequencing of sporadic ccRCC revealed variants in chromatin remodeling genes in addition to *VHL* mutations; variants of *PBRM1*, *BAP1* and *SETD2* were observed in 31, 10 and 11% of sporadic ccRCC, respectively (27,29,30). In our study, although very few variants were commonly observed in 29 BHD-associated kidney cancers, variants in chromatin remodeling genes were observed in 59% of cases over all, indicating that mutations in chromatin remodeling genes might be critical drivers for renal tumorigenesis under *FLCN*-deficiency. Because *Vhl/Bap1* and *Vhl/Pbrm1* doubly inactivated murine kidneys developed kidney cancer (31,32), it would be interesting to investigate whether a mouse doubly deficient for *Flcn* and chromatin remodeling genes develops kidney cancer. The cancer epigenome, which remodels transcription towards cancer development, is highlighted as a target for novel cancer therapeutics (33). Because BHD-associated kidney cancer harbors frequent variants in chromatin remodeling genes, the cancer epigenome would be a promising target for the treatment of BHD-associated kidney cancer.

Vhl knockout mice that exhibited modest cystic changes without cancer formation develop kidney cancer when crossed with *Pbrm1* or *Bap1* knockout mice (31,32). On the other hand, murine *Tsc2* heterozygotes develop cystadenomas with papillary projections by 6–12 months of age, indicating that *TSC2* alterations alone can trigger aberrant kidney cell proliferation and act as strong driver mutations (34). Next generation sequencing of *TSC*-associated kidney cancer revealed a multitude of second hit events in the absence of common variants in genes such as *PBRM1* or *BAP1* whose variants are frequently observed in sporadic ccRCC cases (35). Kidney-specific *Flcn* knockout mice develop highly proliferative polycystic kidneys with 10 times heavier weight compared with control kidneys, suggesting that the *FLCN* alteration alone could trigger aberrant kidney cell proliferation and act as a strong driver mutation (21). In this study, BHD-associated kidney cancer did not display any

Pathway	Patient No.	1		2												3	4	5	6		7	8	9			10	11	12	13	14	15
	Tumor No.	4T3	4T4	59T8	59T10	59T11	59T1	59T2	59T3	59T4	59T6	59T12	59T14	59T15		24T1	35T1	38T1	42T1	42T2	43T1	51T1	19T1	19T2	19T3	98T1	44T1	107T1	15T1	76T1	85T1
	Histology	Ho	Ho	Ho	Ho	Ho	Ch	Ch	Ch	Ch	Ch	Ch	Ch	Ch	Ch	Ch	Ch	Ch	Ch	Ch	Ch	Ch	HC	HC	HC	On	Cl	Cl	Pa	Pa	TP
Mitochondria	ACSS1																			0.1								0.2			
Mitochondria	ADCK4																0.8														
Mitochondria	CISD3																						0.1								
Mitochondria	HAGH																							0.4							
Mitochondria	MSTO1; 2P													0.3																	
Mitochondria	NAGS													0.4																	
Mitochondria	PITRM1	0.6																													
Mitochondria	SMCP																								0.9						
Mitochondria	SMCR7																								0.1						
Mitochondria	TOMM5																1														
Lipid metabolism	ABCA1						1																								
Lipid metabolism	ALOX12B													0.4																	
Lipid metabolism	ATP11B																											0.5			
Lipid metabolism	BSCL2																											0.3			
Lipid metabolism	CES2																0.5														
Lipid metabolism	CYP46A1																										1				
Lipid metabolism	ESYT1													0.4																	
Lipid metabolism	LGALS12						1																								
Lipid metabolism	PLA2G16																								0.4						
Lipid metabolism	PXMP4	0.1																													
Lipid metabolism	SLC27A5													0.4																	
Lipid metabolism	ZNF385A																											0.5			
NADPH	NOXO1									1																					
NADPH	POR																													0.3	
Glycolysis	ADCY5			1																											
Glycolysis	ENO1																				0.9										
Amino acid metabolism	GCN1L1															0.3															
Amino acid metabolism	SLC1A4																													0.4	
Amino acid metabolism	SLC38A10																0.5														
Amino acid metabolism	SLC7A6					1																									
Amino acid metabolism	WDR59																	1													
Autophagy	C9orf72																					0.9									
Autophagy	MAN2B1																								0.3						
Autophagy	NAA30													0.5																	
Autophagy	TFE3										0.5																				
Autophagy	UBQLN2							0.5																							
Autophagy	VMP1													0.8																	

Figure 5. Somatic variants observed in BHD-associated kidney cancer in genes associated with metabolism including mitochondrial metabolism, lipid metabolism, NADPH metabolism, glycolysis, amino acid metabolism and autophagy. Ho, HOCT; Ch, chRCC; HC, HOCT or Ch not determined owing to postmortem degradation; On, Oncocytoma; Cl, ccRCC; Pa, pRCC; TP, tubulopapillary renal cell carcinoma. Values indicate allele frequencies of variants adjusted by tumor purity calculated by an in-house genotyper, Karkinos4.1.11 (23).

variant in genes such as *PBRM1* or *BAP1* whose variants are frequently observed in sporadic ccRCC cases (35) (Supplementary Material, Figs S1 and S2). Taken together, these data suggest that *FLCN* or *TSC2* mutations alone can trigger aberrant kidney cell proliferation leading to tumorigenesis and may not necessarily cooperate with mutations in other specific genes such as *PBRM1* and *BAP1* whose variants are more frequently observed in sporadic ccRCC cases.

Kidney cancer associated genes, *VHL*, *MET*, *FLCN*, *MITF*, *TFE3*, *TFEB*, *TSC1*, *TSC2*, *PTEN*, *FH*, *SDHB* and *SDHD*, are involved in the ability of cells to sense oxygen, iron and nutrients, and broadly regulate metabolic pathways for energy production including mitochondrial oxidative metabolism, glycolysis and autophagy (36). In this study, we observed upregulation of the pentose phosphate pathway which consequently facilitates redox regulation by producing NADPH for neutralizing reactive oxygen species from increased oxidative phosphorylation as well as promotes nucleotide biosynthesis to meet increased demand for cell proliferation. The glutathione synthetic pathway, another important antioxidant pathway, was upregulated in BHD-associated kidney cancer. Taken together with the fact that *FLCN*-deficiency drives increased mitochondrial biogenesis with increased respiratory capacity (10,37), these data suggest that *FLCN*-deficient tumor cells might upregulate redox regulation in order to protect them from reactive oxygen species potentially produced from abundant mitochondria with increased respiratory capacity under *FLCN*-deficiency.

The findings of this study, which delineate the genomic and metabolic landscape of BHD-associated kidney cancer further our understanding of the role of *FLCN* in renal tumor suppression and underscore the molecular pathogenesis of BHD-associated kidney cancer. These data may lead to the development of novel diagnostics and therapeutics for kidney cancer.

Materials and Methods

Patients and tumor histology

Patients known or suspected to be affected with BHD syndrome were evaluated in the Department of Urology and Department

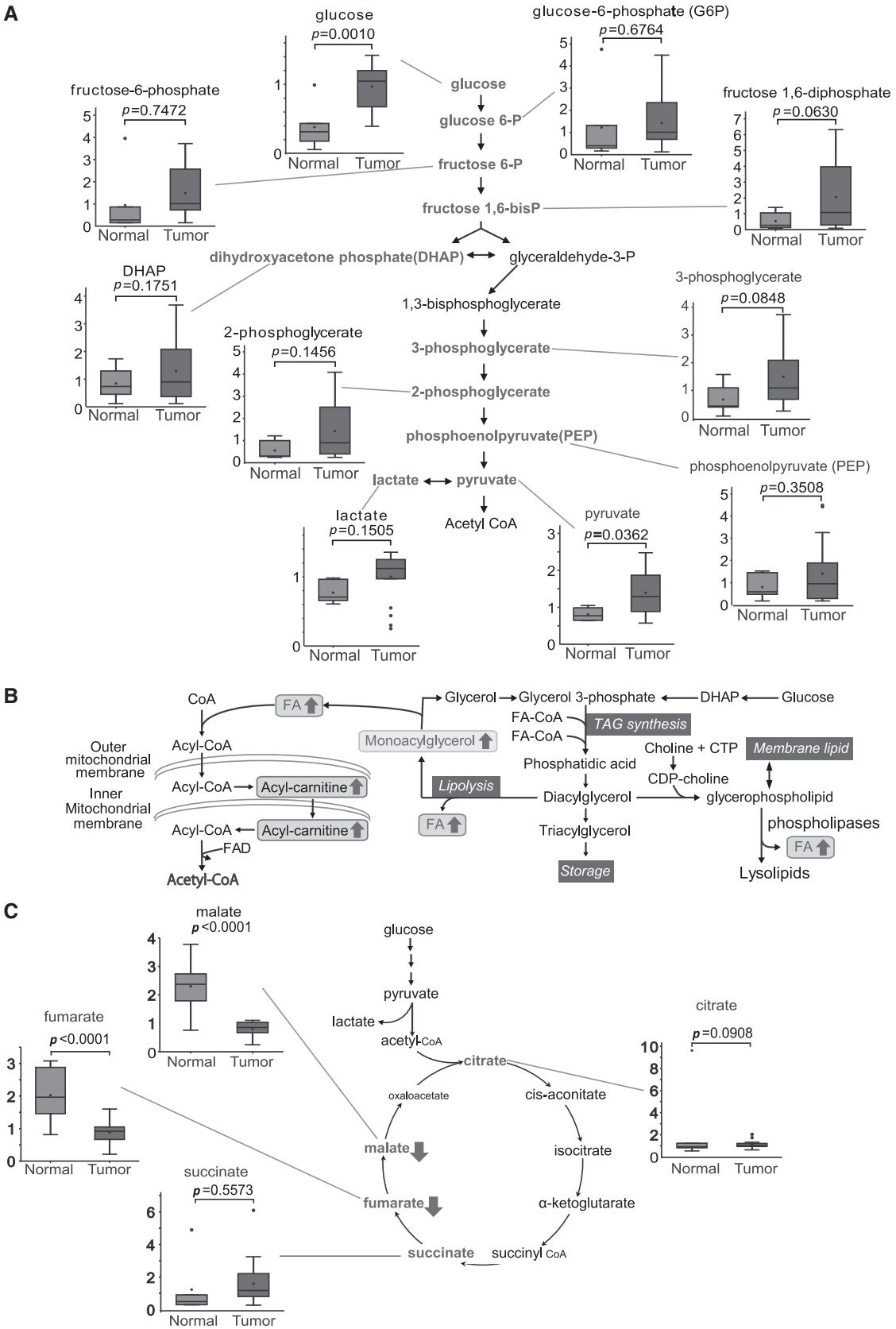

Figure 6. Metabolic reprogramming in BHD-associated kidney cancer. (A) Metabolites in gycolytic pathway. (B) A scheme of the increased transportation of fatty acids into mitochondria. (C) Metabolites in TCA cycle. Blue or red square box represents data of adjacent normal kidney (normal) or BHD-associated kidney cancer (tumor), respectively. Y-axis represents arbitrary unit of signal intensity detected in LC/MS spectrometry. Upper or lower edge of square box indicates upper or lower quartile, respectively. Upper or lower whisker indicates maximum or minimum of distribution, respectively. Plus indicates mean value. Line inside square box indicates median value. White dot indicates extreme data points. Welch's two sample t-test was applied to determine whether the means of two populations are different.

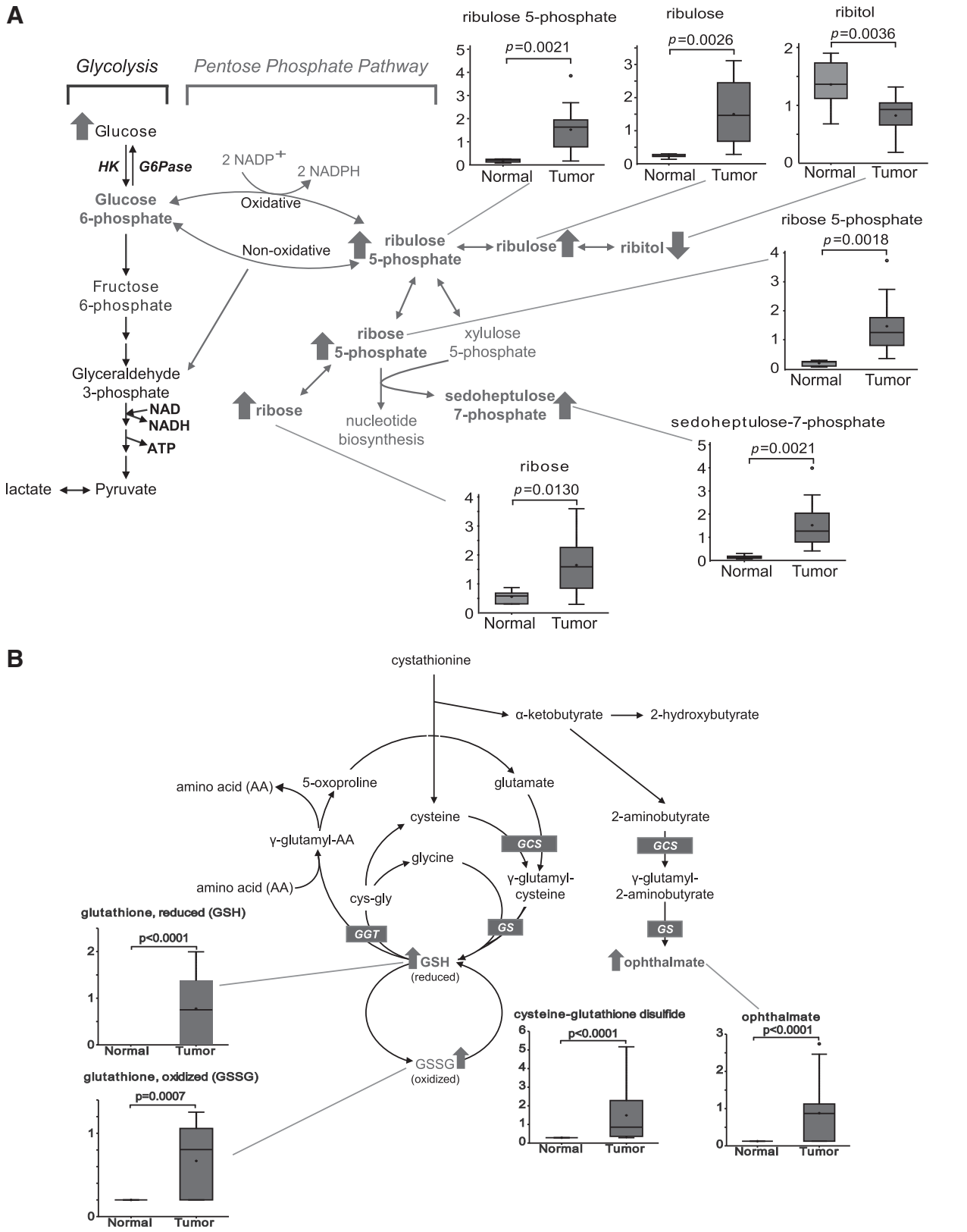

Figure 7. Upregulated redox regulation in BHD-associated kidney cancer. (**A**) Metabolites in pentose phosphate pathway. (**B**) Metabolites in glutathione synthetic pathway. Reduced GSH was not detected in normal kidney. Y-axis represents arbitrary unit of signal intensity detected in LC/MS spectrometry. Blue or red square box represents data of adjacent normal kidney (normal) or BHD-associated kidney cancer (tumor), respectively. Upper or lower edge of square box indicates upper or lower quartile, respectively. Upper or lower whisker indicates maximum or minimum of distribution, respectively. Plus indicates mean value. Line inside square box indicates median value. White dot indicates extreme data points. Welch's two sample *t*-test was applied to determine whether the means of two populations are different. Free fatty acids, monoacylglycerols and acyl-carnitines.

of Molecular Pathology, Yokohama City University, Yokohama 236-0004, Japan, or in the Urologic Oncology Branch, Center for Cancer Research, National Cancer Institute. Some of the BHD-associated tumors in this study were analyzed with SNP array or TFE3 immunohistochemistry analysis and reported previously (38,39). Each patient received genetics counseling and was evaluated for clinical manifestations of BHD syndrome with a dermatologic examination, computed tomography scan and magnetic resonance imaging. Either radical or partial nephrectomy was performed. Resected tissues were fixed with 10% buffered formalin and embedded in paraffin. Hematoxylin and eosin staining and immunostaining were carried out for histologic diagnosis according to our previous study (40). The remaining BHD-associated kidney cancer and adjacent normal kidney samples were frozen with liquid nitrogen and stored in a −80°C freezer until analysis. This work was approved by the ethic committee of Yokohama City University as well as by the NIH Institutional Review Board under protocol no. 02-0159, and each patient was provided written informed consent for publication.

Whole-exome sequencing

Whole-exome sequencing of BHD-associated kidney cancer, adjacent normal kidney and peripheral blood lymphocytes was performed using SureSelect v.5 + lncRNA kit (Agilent) and Illumina HiSeq2000 platform with the 100-bp paired-end read option. Base calling was done using RTA (Real-time-Analysis, Illumina) and Demultiplex was carried out using CASAVA1.8.2 (Illumina). Reads were mapped to the human reference genome using Burrows–Wheeler Aligner (BWA) (41) and Novoalign software independently. Reads with a minimal editing distance to the reference genome were taken to represent optimal alignments. Bam files were locally realigned with SRMA. Because the sequencing data of normal kidney and peripheral blood lymphocytes were almost identical, normal kidney–kidney tumor pair bam files were processed using an in-house genotyper, Karkinos4.1.11, which calculates allele frequencies with cut-off value of 0.05 (23). For the sake of visibility, values of allele frequencies were rounded to the nearest values in figures, and the values before being rounded were provided in the Supplementary Material, Excel file. All the whole-exome sequencing data in this study were deposited at the web site of P-DIRECT (42) under study number 'JGAS000000000115'. All of somatic variants in this study obtained by Karkinos4.1.11 software (23) were available at excel file in Supplementary Material.

Metabolite analyses

Metabolite profiling analyses using LC/MS and GC/MS were carried out in collaboration with Metabolon, Inc. (Durham, NC, USA). Eighteen BHD-associated kidney tumors and six adjacent normal kidneys were prepared for analysis using Metabolon's proprietary solvent extraction method. The extracted supernatant was split into equal parts for analysis on the GC, LC+ and LC− platforms. Signal intensity obtained through LC/MS and GC/MS was normalized to protein concentration determined by Bradford protein assays and described in relative units. A total of 288 biochemicals were detected and among these biochemicals, 91 biochemicals were significantly increased and 72 biochemicals were significantly decreased in BHD-associated kidney cancer compared with adjacent normal kidney.

Statistical analysis

For metabolite analysis, Welch's two sample t-test was applied to determine whether the means of two populations were different, and differences were considered to be statistically significant at a value of $P < 0.05$.

Supplementary Material

Supplementary Material is available at *HMG* online.

Acknowledgements

We thank outside institutes which provided clinical information of BHD patients. We thank Dr Hiromi Soeda in Department of Molecular Pathology, Yokohama City University for her excellent work in Sanger sequencing.

Conflict of Interest statement. None declared.

Funding

The data used in this research is originally obtained through the project in the Project for Development of Innovative Research on Cancer Therapeutics (P-DIRECT)/Ministry of Education, Culture, Sports, Science and Technology of Japan (42) and was provided through the website of the National Bioscience Database Center (NBDC)/the Japan Science and Technology Agency (JST) (43). Authors were supported by JSPS KAKENHI Grant Number as following; H.H. by 16K11020, M.B. by 15604475 and 15551829, M.Y. by 15K10600. This work was also supported by the Intramural Research Program of the National Institutes of Health (NIH), National Cancer Institute (NCI) and Center for Cancer Research. This project was funded in part with federal funds from the Frederick National Laboratory for Cancer Research, NIH, under Contract HHSN261200800001E. The content of this publication does not necessarily reflect the views or policies of the Department of Health and Human Services, nor does mention of trade names, commercial products or organizations imply endorsement by the US Government.

References

1. Hasumi, H., Baba, M., Hasumi, Y., Furuya, M. and Yao, M. (2016) Birt–Hogg–Dube syndrome: clinical and molecular aspects of recently identified kidney cancer syndrome. *Int. J. Urol.*, **23**, 204–210.
2. Furuya, M., Yao, M., Tanaka, R., Nagashima, Y., Kuroda, N., Hasumi, H., Baba, M., Matsushima, J., Nomura, F. and Nakatani, Y. (2016) Genetic, epidemiologic and clinicopathologic studies of Japanese Asian patients with Birt–Hogg–Dube syndrome. *Clin. Genet.*, **90**, 403–412.
3. Nickerson, M.L., Warren, M.B., Toro, J.R., Matrosova, V., Glenn, G., Turner, M.L., Duray, P., Merino, M., Choyke, P., Pavlovich, C.P. *et al.* (2002) Mutations in a novel gene lead to kidney tumors, lung wall defects, and benign tumors of the hair follicle in patients with the Birt–Hogg–Dube syndrome. *Cancer Cell*, **2**, 157–164.
4. Hasumi, H., Hasumi, Y., Baba, M., Nishi, H., Furuya, M., Vocke, C.D., Lang, M., Irie, N., Esumi, C., Merino, M.J. *et al.* (2017) H255Y and K508R missense mutations in tumour suppressor folliculin (FLCN) promote kidney cell proliferation. *Hum. Mol. Genet.*, **26**, 354–366.

5. Vocke, C.D., Yang, Y., Pavlovich, C.P., Schmidt, L.S., Nickerson, M.L., Torres-Cabala, C.A., Merino, M.J., Walther, M.M., Zbar, B. and Linehan, W.M. (2005) High frequency of somatic frameshift BHD gene mutations in Birt–Hogg–Dube-associated renal tumors. *J. Natl. Cancer Inst.*, **97**, 931–935.
6. Possik, E., Ajisebutu, A., Manteghi, S., Gingras, M.C., Vijayaraghavan, T., Flamand, M., Coull, B., Schmeisser, K., Duchaine, T., van Steensel, M. *et al.* (2015) FLCN and AMPK confer resistance to hyperosmotic stress via remodeling of glycogen stores. *PLoS Genet.*, **11**, e1005520.
7. Possik, E., Jalali, Z., Nouet, Y., Yan, M., Gingras, M.C., Schmeisser, K., Panaite, L., Dupuy, F., Kharitidi, D., Chotard, L. *et al.* (2014) Folliculin regulates AMPK-dependent autophagy and metabolic stress survival. *PLoS Genet.*, **10**, e1004273.
8. Hartman, T.R., Nicolas, E., Klein-Szanto, A., Al-Saleem, T., Cash, T.P., Simon, M.C. and Henske, E.P. (2009) The role of the Birt–Hogg–Dube protein in mTOR activation and renal tumorigenesis. *Oncogene*, **28**, 1594–1604.
9. Hasumi, Y., Baba, M., Hasumi, H., Huang, Y., Lang, M., Reindorf, R., Oh, H.B., Sciarretta, S., Nagashima, K., Haines, D.C. *et al.* (2014) Folliculin (Flcn) inactivation leads to murine cardiac hypertrophy through mTORC1 deregulation. *Hum. Mol. Genet.*, **23**, 5706–5719.
10. Hasumi, H., Baba, M., Hasumi, Y., Huang, Y., Oh, H., Hughes, R.M., Klein, M.E., Takikita, S., Nagashima, K., Schmidt, L.S. and Linehan, W.M. (2012) Regulation of mitochondrial oxidative metabolism by tumor suppressor FLCN. *J. Natl. Cancer Inst.*, **104**, 1750–1764.
11. Yan, M., Gingras, M.C., Dunlop, E.A., Nouet, Y., Dupuy, F., Jalali, Z., Possik, E., Coull, B.J., Kharitidi, D., Dydensborg, A.B. *et al.* (2014) The tumor suppressor folliculin regulates AMPK-dependent metabolic transformation. *J. Clin. Invest.*, **124**, 2640–2650.
12. Baba, M., Toyama, H., Sun, L., Takubo, K., Suh, H.C., Hasumi, H., Nakamura-Ishizu, A., Hasumi, Y., Klarmann, K.D., Nakagata, N. *et al.* (2016) Loss of folliculin disrupts hematopoietic stem cell quiescence and homeostasis resulting in bone marrow failure. *Stem Cells*, **34**, 1068–1082.
13. Wada, S., Neinast, M., Jang, C., Ibrahim, Y.H., Lee, G., Babu, A., Li, J., Hoshino, A., Rowe, G.C., Rhee, J. *et al.* (2016) The tumor suppressor FLCN mediates an alternate mTOR pathway to regulate browning of adipose tissue. *Genes Dev.*, **30**, 2551–2564.
14. Khabibullin, D., Medvetz, D.A., Pinilla, M., Hariharan, V., Li, C., Hergrueter, A., Laucho Contreras, M., Zhang, E., Parkhitko, A., Yu, J.J. *et al.* (2014) Folliculin regulates cell-cell adhesion, AMPK, and mTORC1 in a cell-type-specific manner in lung-derived cells. *Physiol Rep.*, **2**, e12107–e12116.
15. Baba, M., Keller, J.R., Sun, H.W., Resch, W., Kuchen, S., Suh, H.C., Hasumi, H., Hasumi, Y., Kieffer-Kwon, K.R., Gonzalez, C.G. *et al.* (2012) The folliculin-FNIP1 pathway deleted in human Birt–Hogg–Dube syndrome is required for murine B-cell development. *Blood*, **120**, 1254–1261.
16. Baba, M., Hong, S.B., Sharma, N., Warren, M.B., Nickerson, M.L., Iwamatsu, A., Esposito, D., Gillette, W.K., Hopkins, R.F., 3rd, Hartley, J.L. *et al.* (2006) Folliculin encoded by the BHD gene interacts with a binding protein, FNIP1, and AMPK, and is involved in AMPK and mTOR signaling. *Proc. Natl. Acad. Sci. USA.*, **103**, 15552–15557.
17. Hasumi, H., Baba, M., Hong, S.B., Hasumi, Y., Huang, Y., Yao, M., Valera, V.A., Linehan, W.M. and Schmidt, L.S. (2008) Identification and characterization of a novel folliculin-interacting protein FNIP2. *Gene*, **415**, 60–67.
18. Hasumi, H., Baba, M., Hasumi, Y., Lang, M., Huang, Y., Oh, H.F., Matsuo, M., Merino, M.J., Yao, M., Ito, Y. *et al.* (2015) Folliculin-interacting proteins Fnip1 and Fnip2 play critical roles in kidney tumor suppression in cooperation with Flcn. *Proc. Natl. Acad. Sci. USA.*, **112**, E1624–E1631.
19. Nagashima, K., Fukushima, H., Shimizu, K., Yamada, A., Hidaka, M., Hasumi, H., Ikebe, T., Fukumoto, S., Okabe, K. and Inuzuka, H. (2017) Nutrient-induced FNIP degradation by SCFbeta-TRCP regulates FLCN complex localization and promotes renal cancer progression. *Oncotarget*, **8**, 9947–9960.
20. Hasumi, Y., Baba, M., Ajima, R., Hasumi, H., Valera, V.A., Klein, M.E., Haines, D.C., Merino, M.J., Hong, S.B., Yamaguchi, T.P. *et al.* (2009) Homozygous loss of BHD causes early embryonic lethality and kidney tumor development with activation of mTORC1 and mTORC2. *Proc. Natl. Acad. Sci. USA.*, **106**, 18722–18727.
21. Baba, M., Furihata, M., Hong, S.B., Tessarollo, L., Haines, D.C., Southon, E., Patel, V., Igarashi, P., Alvord, W.G., Leighty, R. *et al.* (2008) Kidney-targeted Birt–Hogg–Dube gene inactivation in a mouse model: Erk1/2 and Akt-mTOR activation, cell hyperproliferation, and polycystic kidneys. *J. Natl. Cancer Inst.*, **100**, 140–154.
22. Yao, M., Latif, F., Orcutt, M.L., Kuzmin, I., Stackhouse, T., Zhou, F.W., Tory, K., Duh, F.M., Richards, F. and Maher, E. (1993) von Hippel-Lindau disease: identification of deletion mutations by pulsed-field gel electrophoresis. *Hum. Genet.*, **92**, 605–614.
23. Ueda, H. Karkinos software; tumor genotyper for exome sequencing that detects SNV, CNV and tumor purity. https://sourceforge.net/projects/karkinos/ (accessed 20 February 2017).
24. Durinck, S., Stawiski, E.W., Pavia-Jimenez, A., Modrusan, Z., Kapur, P., Jaiswal, B.S., Zhang, N., Toffessi-Tcheuyap, V., Nguyen, T.T., Pahuja, K.B. *et al.* (2015) Spectrum of diverse genomic alterations define non-clear cell renal carcinoma subtypes. *Nat. Genet.*, **47**, 13–21.
25. Davis, C.F., Ricketts, C.J., Wang, M., Yang, L., Cherniack, A.D., Shen, H., Buhay, C., Kang, H., Kim, S.C., Fahey, C.C. *et al.* (2014) The somatic genomic landscape of chromophobe renal cell carcinoma. *Cancer Cell*, **26**, 319–330.
26. Sato, Y., Yoshizato, T., Shiraishi, Y., Maekawa, S., Okuno, Y., Kamura, T., Shimamura, T., Sato-Otsubo, A., Nagae, G., Suzuki, H. *et al.* (2013) Integrated molecular analysis of clear-cell renal cell carcinoma. *Nat. Genet.*, **45**, 860–867.
27. Cancer Genome Atlas Research Network. (2013) Comprehensive molecular characterization of clear cell renal cell carcinoma. *Nature*, **499**, 43–49.
28. Linehan, W.M., Spellman, P.T., Ricketts, C.J., Creighton, C.J., Fei, S.S., Davis, C., Wheeler, D.A., Murray, B.A., Schmidt, L., Vocke, C.D. *et al.* (2016) Comprehensive molecular characterization of papillary renal-cell carcinoma. *N. Engl. J. Med.*, **374**, 135–145.
29. Brugarolas, J. (2014) Molecular genetics of clear-cell renal cell carcinoma. *J. Clin. Oncol.*, **32**, 1968–1976.
30. Pena-Llopis, S., Vega-Rubin-de-Celis, S., Liao, A., Leng, N., Pavia-Jimenez, A., Wang, S., Yamasaki, T., Zhrebker, L., Sivanand, S., Spence, P. *et al.* (2012) BAP1 loss defines a new class of renal cell carcinoma. *Nat. Genet.*, **44**, 751–759.
31. Wang, S.S., Gu, Y.F., Wolff, N., Stefanius, K., Christie, A., Dey, A., Hammer, R.E., Xie, X.J., Rakheja, D., Pedrosa, I. *et al.* (2014) Bap1 is essential for kidney function and cooperates with Vhl in renal tumorigenesis. *Proc. Natl. Acad. Sci. USA.*, **111**, 16538–16543.

32. Nargund, A.M., Pham, C.G., Dong, Y., Wang, P.I., Osmangeyoglu, H.U., Xie, Y., Aras, O., Han, S., Oyama, T., Takeda, S. *et al.* (2017) The SWI/SNF protein PBRM1 restrains VHL-loss-driven clear cell renal cell carcinoma. *Cell Rep.*, **18**, 2893–2906.
33. Kronfol, M.M., Dozmorov, M.G., Huang, R., Slattum, P.W. and McClay, J.L. (2017) The role of epigenomics in personalized medicine. *Expert Rev. Precis Med. Drug Dev.*, **2**, 33–45.
34. Onda, H., Lueck, A., Marks, P.W., Warren, H.B. and Kwiatkowski, D.J. (1999) Tsc2(+/−) mice develop tumors in multiple sites that express gelsolin and are influenced by genetic background. *J. Clin. Invest.*, **104**, 687–695.
35. Tyburczy, M.E., Jozwiak, S., Malinowska, I.A., Chekaluk, Y., Pugh, T.J., Wu, C.L., Nussbaum, R.L., Seepo, S., Dzik, T., Kotulska, K. and Kwiatkowski, D.J. (2015) A shower of second hit events as the cause of multifocal renal cell carcinoma in tuberous sclerosis complex. *Hum. Mol. Genet.*, **24**, 1836–1842.
36. Linehan, W.M. and Ricketts, C.J. (2013) The metabolic basis of kidney cancer. *Semin. Cancer Biol.*, **23**, 46–55.
37. Yan, M., Audet-Walsh, E., Manteghi, S., Dufour, C.R., Walker, B., Baba, M., St-Pierre, J., Giguere, V. and Pause, A. (2016) Chronic AMPK activation via loss of FLCN induces functional beige adipose tissue through PGC-1alpha/ERRalpha. *Genes Dev.*, **30**, 1034–1046.
38. Furuya, M., Hong, S.B., Tanaka, R., Kuroda, N., Nagashima, Y., Nagahama, K., Suyama, T., Yao, M. and Nakatani, Y. (2015) Distinctive expression patterns of glycoprotein non-metastatic B and folliculin in renal tumors in patients with Birt–Hogg–Dube syndrome. *Cancer Sci.*, **106**, 315–323.
39. Iribe, Y., Yao, M., Tanaka, R., Kuroda, N., Nagashima, Y., Nakatani, Y. and Furuya, M. (2016) Genome-wide uniparental disomy and copy number variations in renal cell carcinomas associated with Birt–Hogg–Dube syndrome. *Am. J. Pathol.*, **186**, 337–346.
40. Iribe, Y., Kuroda, N., Nagashima, Y., Yao, M., Tanaka, R., Gotoda, H., Kawakami, F., Imamura, Y., Nakamura, Y., Ando, M. *et al.* (2015) Immunohistochemical characterization of renal tumors in patients with Birt–Hogg–Dube syndrome. *Pathol. Int.*, **65**, 126–132.
41. Li, H. and Durbin, R. (2009) Fast and accurate short read alignment with Burrows–Wheeler transform. *Bioinformatics*, **25**, 1754–1760.
42. Project for Development of Innovative Research on Cancer Therapeutics (P-DIRECT). http://p-direct.jfcr.or.jp/english/ (accessed 18 September 2017).
43. Kodama, Y., Mashima, J., Kosuge, T., Katayama, T., Fujisawa, T., Kaminuma, E., Ogasawara, O., Okubo, K., Takagi, T. and Nakamura, Y. (2015) The DDBJ Japanese Genotype-phenotype Archive for genetic and phenotypic human data. *Nucleic Acids Res.*, **43**, D18–D22.